

Faceting of $\Sigma 3$ grain boundaries in Cu: three-dimensional Wulff diagrams

Yaroslav Kucherinenko^{1,a}, Svetlana Protasova^{2,b}, Boris Straumal^{2,c}

¹Geological faculty, Moscow Lomonosov State University, Vorobjovy gory, 119992 Moscow, Russia

²Institute of Solid State Physics, Russian Academy of Sciences, Chernogolovka, Moscow District, 142432 Russia

^akuch@geol.msu.ru, ^bsveta@issp.ac.ru, ^cstraumal@issp.ac.ru

Keywords: Grain boundaries, Faceting, Phase diagrams.

Abstract. Diffusional growth of the grain boundary (GB) groove permits one to measure the ratio between GB energy σ_{GB} and surface energy σ_{sur} . The faceting of twin tilt grain boundaries in Cu has been studied using the GB thermal groove method. No rough facet edges were observed. It means that melting temperature is lower than the roughening temperature for the observed facets in Cu. The influence of orientation and misorientation deviation $\Delta\theta = |\theta - \theta_{\Sigma}|$ from coincidence misorientation θ_{Σ} has been studied. By increase of $\Delta\theta$ the energy of $(100)_{CSL}$ facet increases. The convenient method for construction 3D three-dimensional Wulff diagrams was found. The 3-dimensional Wulff diagrams were constructed using this method and measured $\sigma_{GB} / \sigma_{sur}$ values.

Introduction

The Wulff diagram is the set of ends of radius-vectors, which are perpendicular to all possible (and virtual) faces of a crystal. The length of each vector is equal to surface energy of the corresponding face of a crystal (Fig. 1). This diagram can be called “polar” in two-dimensional case, and “spherical” in three-dimensional cases. Similarly to the Wulff diagrams for the free surface of a crystal, it is possible to consider Wulff diagrams for grain boundaries (GBs). In GB cases one has to assume that the misorientation of both grains forming a GB is fixed, and the orientation (inclination) of a flat GB can vary. To different misorientations of a GB correspond different Wulff diagrams.

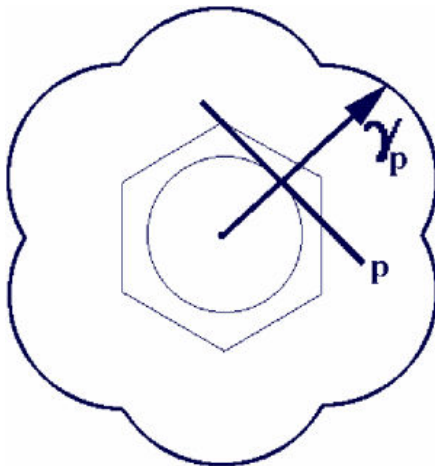


Fig. 1. Definition of a Wulff diagram. For an arbitrary plane p we consider the end of its surface energy vector. The Wulff diagram is a set of such points, constructed for all plane orientations.

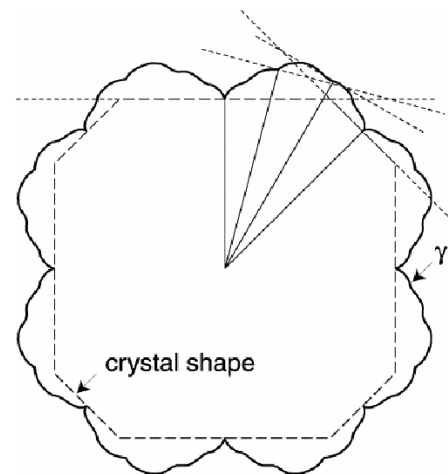


Fig. 2. Construction of equilibrium crystal shape from Wulff diagram by envelope planes.

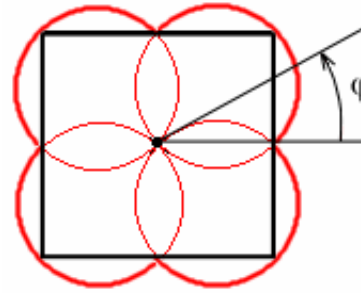
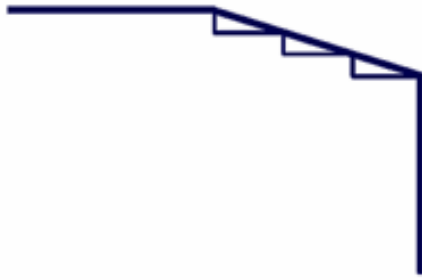


Fig. 3a. One face of a crystal is composed of more stable faces.

Fig. 3b. Function of surface energy for a two-dimensional square crystal $\gamma = |\cos\phi| + |\sin\phi|$.

Wulff diagrams not only allow to find a surface energy for any crystal faces, but also make possible to construct an equilibrium crystal shape (ECS). Landau has shown, that the ECS is an intersection of half-subspaces, bounded by envelope planes (Fig. 2) [1]. Studying of energy diagrams was begun by works of P. Ehrenfest and G. Wulff [2, 3] and continued by C. Herring [4]. Ehrenfest has proved an opportunity of occurrence of such faces in real crystals, which deviate from the most stable planes insignificantly. He has shown it using an example of a two-dimensional tetragonal crystal. Ehrenfest has deduced function of surface energy of such crystal (Fig. 3b), assuming that faces of less favorable directions are formed by steps of more stable ones (Fig. 4a).

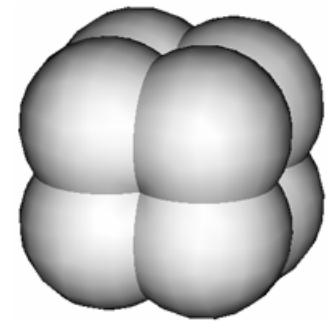
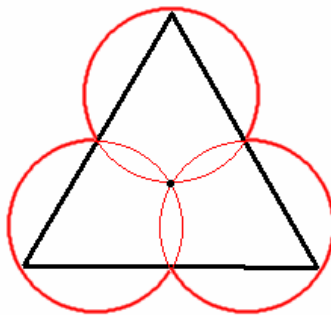
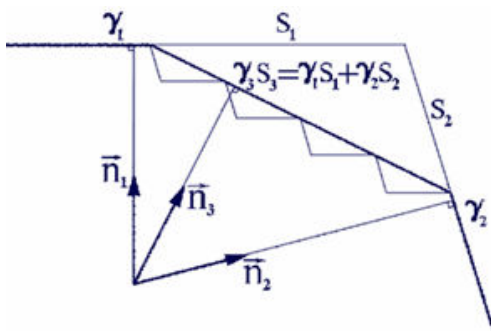


Fig. 4a. One face of crystal is composed of steps of more stable faces. Oblique-angled case.

Fig. 4b. Function of surface energy for a three-trigonal crystal.

Fig. 4c. Wulff diagram of surface energy for a three-dimensional cubic crystal.

As a result, the function of surface energy in polar coordinates is a hull enveloping four circles. Each of these four circles passes through the origin of coordinates. The envelope consists of four circular arcs. If a crystal face slightly deviates from the most favorable orientation, its energy deviates also slightly from the respective energy. Wulff [2, 3] has generalized a design offered earlier by Ehrenfest for crystals of any syngony (Fig. 4a), including a three-dimensional case. The result is rather similar to the previous one: function of surface energy in polar (spherical) coordinates is a hull enveloping some circles (Fig. 4b) or spheres (Fig. 4c) which includes origin of coordinates.

Method for constructing Wulff diagrams

The method developed in this work is based on an important property of geometric transformation, inversion in a circle or sphere (Fig. 5a). Circles (or spheres) including the origin of coordinates are transformed by inversion into straight lines (planes) (Fig. 5b). A Wulff diagram consisting of fragments of circles (or spheres) is transformed, respectively, into a convex polygon (or polyhedron) (Fig. 5c). Convexity of a polyhedron follows from a simple physical reason: if a polyhedron would be not convex, it would have re-entrant corners, and the Wulff diagram would have a maximum at a point of crossing of corresponding arcs of circles, while there should be a minimum.

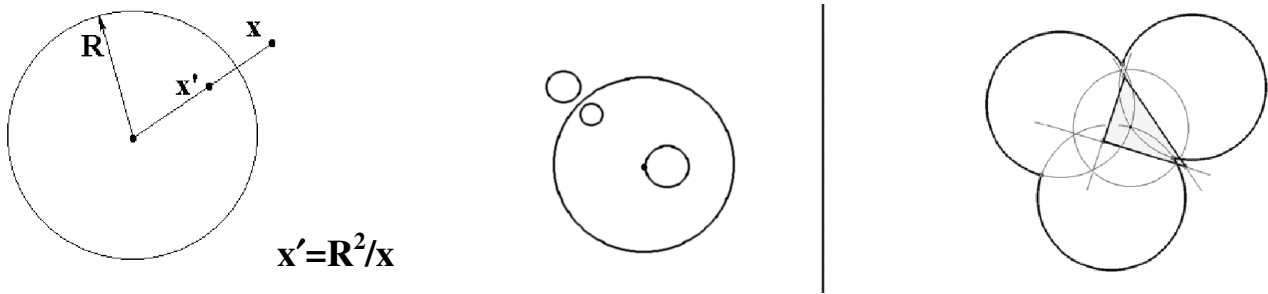


Fig. 5a. Definition of inversion in a circle (sphere): the point having distance x from the origin passes into a point x' , lying on the same straight line.

Fig. 5b. Property of inversion: a circle which includes the origin of coordinates, transforms into a straight line (i.e. a circle with an infinite radius).

Fig. 5c. The Wulff diagram, consisting of three circular fragments, passes into triangle.

We propose the following method for the construction of Wulff diagrams. Step 1. One constructs the radius vectors normal to all stable faces of a crystal. The lengths of these vectors correspond to the surface energies (Fig. 6a). Step 2. The inversion transformation in a circle (sphere) is applied to the set of points received in the Step 1 (Fig. 6b). If the transformation sphere is of unit radius $R = 1$, the radius vectors σ are transformed into inverse ones $1/\sigma$. Step 3. The convex hull of the received set of points are calculated. Result will be a convex polyhedron (Fig. 6c). Step 4. The inversion transformation is applied to the convex polyhedron obtained in the Step 3 in a same sphere as in the Step 2. The result is a Wulff diagram.

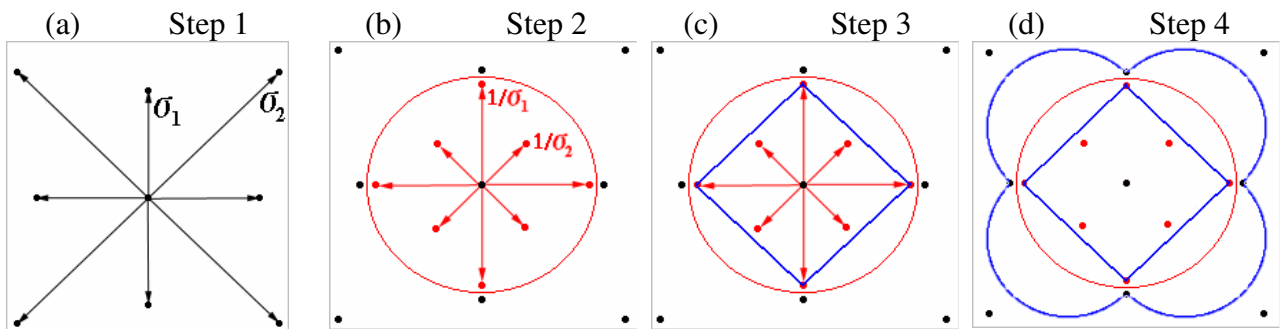


Fig. 6. Construction of Wulff diagram.

It is possible to construct Wulff diagrams for grain boundary energy in a similar manner to the surface energy, including the cases of slight deviations from equilibrium. But for these cases, the technique of construction of diagrams should be modified by lengthening of initial set of vectors on some fitting parameter r_c (which is independent on orientation) and subtraction of same constant from all radius-vectors of spherical diagram at the final stage. Such modification allows to receive functions on sphere with higher variations of values. Stages of modified method for construction of Wulff diagram are shown in Fig. 7:

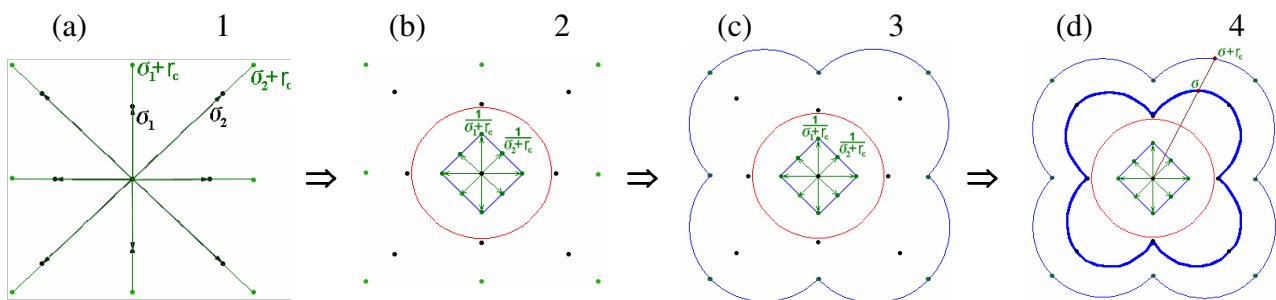


Fig.7. Modified method for the construction of Wulff diagram.

Experimental

Experiments on preparation of samples and measurement of grain boundary energy are described in [4]. Two series of $\Sigma 3$ bicrystals corresponding to the tilt GBs with inclinations $\langle 110 \rangle \phi = 0..90^\circ$ and $\langle 211 \rangle \phi = 0..90^\circ$ were prepared by diffusion bonding (Σ is the inverse density of coincidence sites). A cylindrical Cu bicrystal with coaxial grains was also grown. A natural spread in misorientation angle θ of $\Sigma 3$ twin GBs is present in this bicrystal permitting to investigate the shape of Wulff diagram at various θ . The profiles of the formed GB thermal groove were analyzed by atomic force microscope (AFM) after annealing at $T = 1293 \text{ K} = 0.95 T_m$ (T_m is melting temperature). Mullins solution for the diffusion-controlled groove growth has been used for fitting of experimental profile and determination of the ratio between GB energy σ_{GB} and surface energy σ_{sur} .

Results and discussion

No rough facet edges were observed in both sets of experiments at $0.95 T_m$. It means that T_m is lower than the roughening temperature for the observed facets in Cu. Molecular statics calculations for surface energy of faces (110) and (211) which were represented in [5], have allowed to compare two data series of Fig. 8, to represent them on three dimensional spherical diagram (Fig. 9), and to apply the modified method of constructing Wulff diagrams. The optimal values of r_c were 3.0 J/m^2 for simulated data and 1.0 J/m^2 for experimental data.

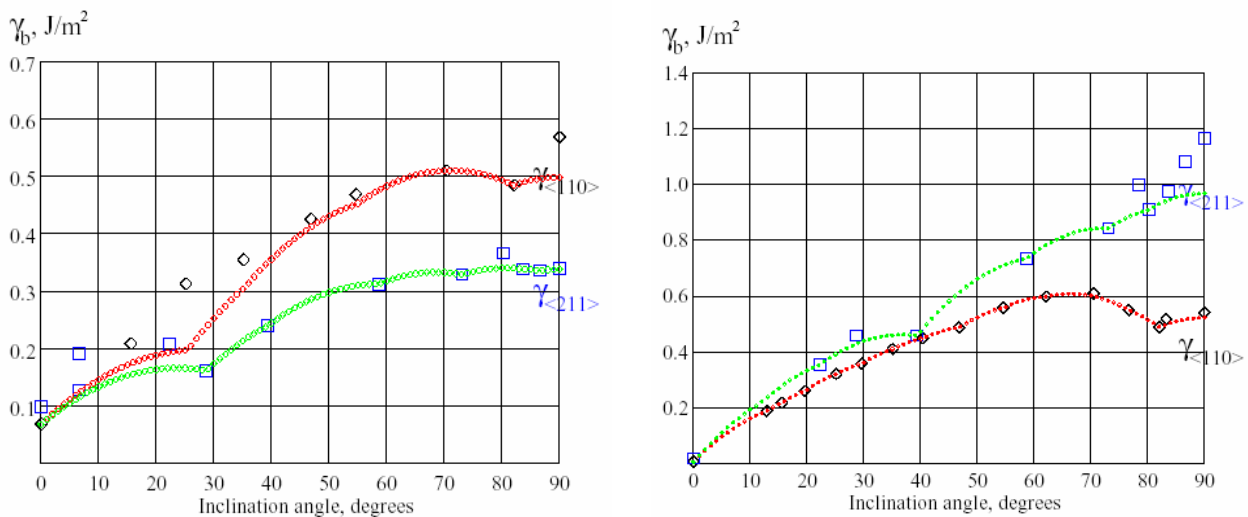


Fig. 8. Dependence of the $\sigma_{GB} / \sigma_{sur}$ ratio on inclination ϕ for the $\langle 110 \rangle$ and $\langle 211 \rangle$ tilt $\Sigma 3$ GBs (a) thermal groove experiments (b) molecular statics calculations.

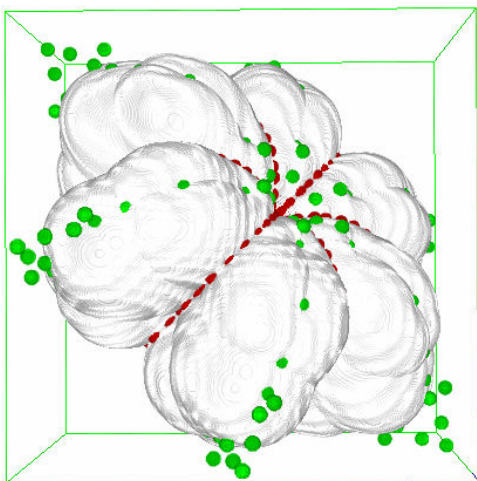
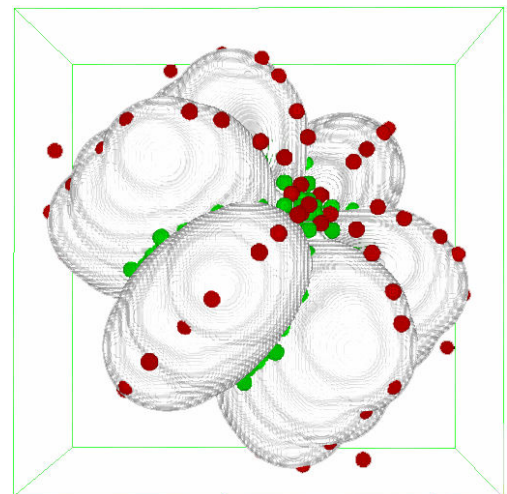
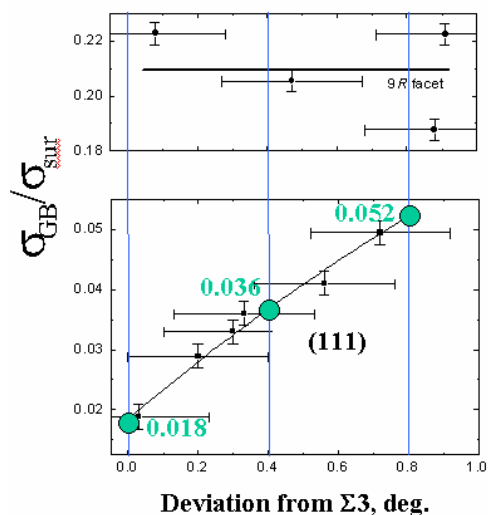


Fig. 9. Three-dimensional Wulff diagrams for grain boundaries $\Sigma 3$ in Cu obtained using the experimental data from Fig. 8 for two orthogonal misorientation axes $\langle 110 \rangle$ and $\langle 211 \rangle$.



Three-dimensional Wulff diagrams for grain boundaries Cu $\Sigma 3$ and their comparison with experimental data are represented in Fig. 9. Further we not consider this point and concurrence was improved. At $0.95 T_m$ $\Sigma 3$ GB contains two facets, namely symmetric twin at $\phi=0^\circ$ and 9R facet at $\phi=82^\circ$. 9R facet does not coincide with any densely packed plane of coincidence sites lattice $\Sigma 3$.



In Fig. 10 the influence of misorientation deviation $\Delta\theta = |\theta - \theta_{\Sigma 3}|$ from coincidence misorientation $\theta_{\Sigma 3}$ on the $\sigma_{GB} / \sigma_{sur}$ ratio is shown. It can be seen that with increasing $\Delta\theta$ the energy of symmetric twin linearly increases, and σ_{GB} for 9R does not change significantly. The data on the $\Delta\theta$ influence have allowed to see the character of change of shape of Wulff diagram (Fig. 11).

Fig. 10. Dependence of the $\sigma_{GB} / \sigma_{sur}$ ratio on misorientation deviation $\Delta\theta$ for symmetric twin and 9R facet. Large points represent interpolated values used for the calculation of Wulff diagrams (Fig. 11).

The 3-dimensional Wulff diagram have been constructed for different $\Delta\theta$. Externally, they are almost indistinguishable (Fig. 11). The data shown in Fig. 10 were used to deform the curves for the $\Delta\theta = 0$ (Fig. 8). Figs 12a to 12c demonstrate the result of this fitting. In Figs 12d to 12f the sections of the resulted 3-dimensional Wulff diagrams are shown. These sections allow one to see the main difference in the shape of Wulff diagrams with increasing $\Delta\theta$. The very low energy of coherent twin facets (thin central “needle” on the Wulff plot) determine the platelet-like shape of twins in Cu. It can be seen that with increasing $\Delta\theta$ the energy of symmetric twin increases, “central needle” shortens, Wulff’s diagram changes and becomes more “spherical”. It means that by further increase of $\Delta\theta$ the transition from faceted to rough GB can occur, similar to that proceeding with increasing temperature.

Acknowledgements

This work was supported by the Russian Foundation of Basic Research (contracts 03-02-16947 and 03-02-04000), INTAS Programme under contract 03-51-3779, NATO Linkage grant (PST.CLG.979375), German Federal Ministry for Education and Research (BMBF) under WTZ-Project RUS 04/014, and exchange programme between Russian and Polish Academies of Sciences.

References

- [1] L.D. Landau and E.M. Lifshitz: Statistical Physics (Pergamon, Oxford 1980), 3rd ed. revised by E.M. Lifshitz, L.P. Pitaevskii, Part 1.
- [2] G. Wulff: Trudy Warsh. obsh. estestvoisp. Vol. 6 (1894), p. 7 (in Russian).
- [3] G. Wulff: Zt. Krystallogr. Vol. 34 (1901), p. 449 (in German).
- [4] C. Herring: Phys. Rev. Vol. 82. (1951) p. 87.
- [5] F. Ernst, M.W. Finnis, A. Koch, C. Schmidt, B. Straumal and W.Gust: Zt. Metallkd. Vol. 87 (1996), p. 911.

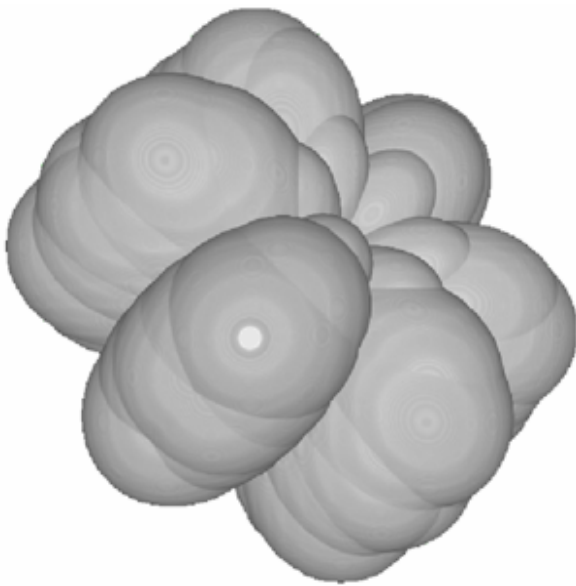


Fig. 11. All Wulff diagrams which have been constructed using experimental data on the $\Delta\theta$ dependence are externally indistinguishable.

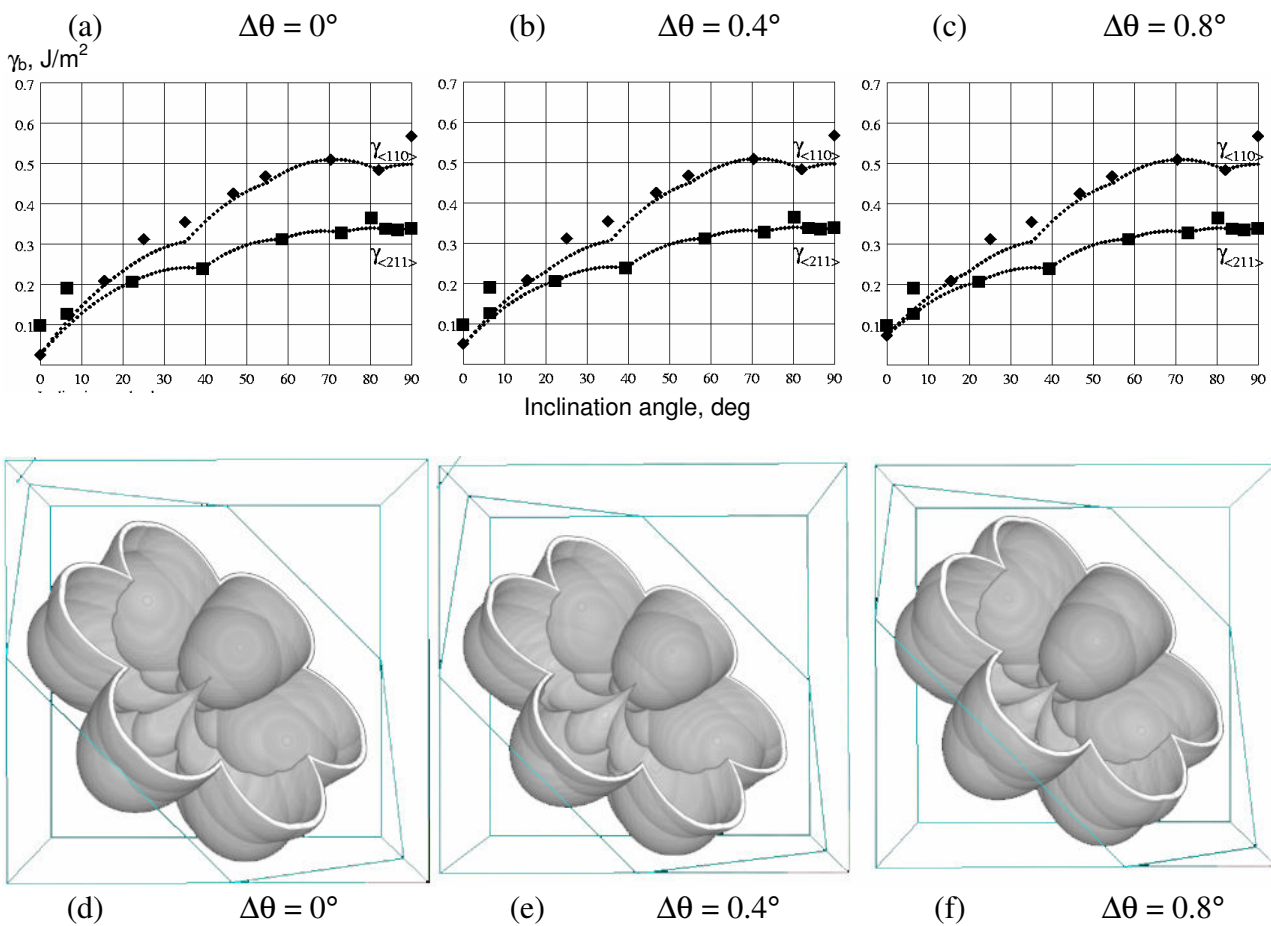


Fig. 12. Dependence of Wulff diagram from deviation from $\Sigma 3$. (a) to (c) Inclination dependences of $\sigma_{GB} / \sigma_{sur}$ ratio for different $\Delta\theta$ values. (d) to (f) Sections of Wulff diagram by the (111) plane for different $\Delta\theta$ values. With increasing deviation $\Delta\theta$ the energy minimum of a facet (111) (central needle) becomes less and less deep.